## Taylor & Francis Taylor & Francis Group

### Transportmetrica A: Transport Science

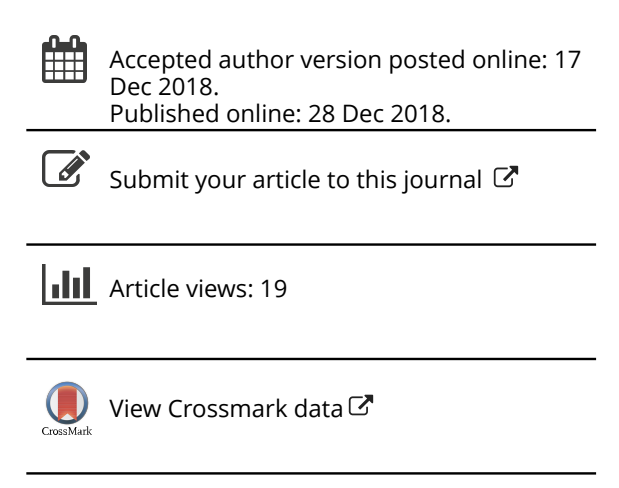
ISSN: 2324-9935 (Print) 2324-9943 (Online) Journal homepage: http://www.tandfonline.com/loi/ttra21

# Two-stage model for optimizing traffic signal control plans of signalized Superstreet

Liu Xu, Xianfeng Yang & Gang-Len Chang

To cite this article: Liu Xu, Xianfeng Yang & Gang-Len Chang (2018): Two-stage model for optimizing traffic signal control plans of signalized Superstreet, Transportmetrica A: Transport Science, DOI: 10.1080/23249935.2018.1559894

To link to this article: <a href="https://doi.org/10.1080/23249935.2018.1559894">https://doi.org/10.1080/23249935.2018.1559894</a>







# Two-stage model for optimizing traffic signal control plans of signalized Superstreet

Liu Xua, Xianfeng Yangb and Gang-Len Changa

<sup>a</sup>Department of Civil & Environmental Engineering, University of Maryland, College Park, MD, USA;

#### **ABSTRACT**

Despite the increasing implementations of Superstreets, a reliable method to design their signal plan remains unavailable. To account for the unique geometric features of Superstreets, this study presents a two-stage signal optimization method where the first stage determines the optimal signal plan for each sub-intersection and the second stage optimizes the offset for signal coordination. Implementing the Mixed-Integer-Linear-Programming (MILP) technique for the model formulation, the first stage has the objective of maximizing total traffic throughput and the second stage aims to maximize the bandwidths and minimize the delay experienced by the minor road drivers. To assess the proposed model's effectiveness, the study further conducts signal performance evaluations using simulation calibrated with field data collected in Maryland. The results of extensive experiment tests reveal that the proposed model can effectively offer signal progressions to both heavy through and left-turn movements, and prevent the potential gueue spillback among a Superstreet's four closely-spaced sub-intersections.

#### **ARTICLE HISTORY**

Received 26 April 2017 Accepted 13 December 2018

#### **KEYWORDS**

Superstreet; signal optimization; throughput maximization; signal coordination

#### 1. Introduction

Superstreet, also known as a restricted crossing U-turn intersection (RCUT), is a promising treatment with markedly lower rate of sideswipe, rear-ends and head-on collisions (Hummer 1998). Differing from a conventional intersection, Superstreet usually restricts the minor road left-turn and through movements to first make right turns, and then allow them to pursue the original directions following a directional U-turn. When signalized, this type of design can provide large, uninterrupted progression bands in both directions along an arterial of heavy traffic volumes. In addition, it only requires two-phase signal control plans which helps reducing intersections' signal lost time.

Due to the increasing applications of Superstreet in recent years, some fundamental issues associated with its operational efficiency have emerged as the priority research subjects in the traffic community (Xu, Yang, and Chang 2017). For example, Reid and Hummer (1999, 2001) pointed out that in terms of operational efficiency, Superstreet can outperform

<sup>&</sup>lt;sup>b</sup>Department of Civil and Environmental Engineering, University of Utah, Salt Lake City, UT, USA

a conventional intersection when the volumes for the left-turn and through movements from minor streets are at the low-medium level. In addition, Hummer et al. (2010) further explored a method to determine the capacity of Superstreets by adjusting the critical lane volume used in HCM. Realizing the lack of sufficient operational guidance, Haley et al. (2011) analyzed the performance of Superstreets by comparing them with equivalent conventional intersections, based on the calibrated simulation results. They reported that it would be effective to adopt a Superstreet design when the arterial's left-turn volume per lane is greater than 80 percent of the volume on the minor roads during the same signal phase. Also, based on the results of simulation-based comparisons, Kim, Chang, and Rahwanji (2007) reported the apparent operational and safety benefits offered by Superstreets under the high-volume conditions.

More recently, as part of the efforts to promote popular unconventional intersection designs, the Federal Highway Administration has offered a series of guides (Hughes et al. 2010; Hummer et al. 2014) to help transportation professionals evaluate a candidate Superstreet implementation with some state of the practices. Aside from improving the operational performance, various studies have also confirmed that Superstreet can help reduce accident rate and alleviate crash severity (Liu 2014; Ott et al. 2012; Thompson and Hummer 2001; Moon et al. 2011). In brief, existing studies have consistently concluded that Superstreet can outperform conventional intersections in terms of operational efficiency, especially when the traffic on its major arterial dominates those from the minor approaches (Naghawi and Idewu 2014; Naghawi, AlSoud, and AlHadidi 2018). Yet, such a desirable operation cannot be achieved without a proper signal plan. With the review of related studies (Zhao et al. 2015; Sun et al. 2016), it is noticeable that the optimal signal strategy to accommodate the heavy arterial flows among the four closely-spaced sub-intersections in a Superstreet remains unavailable. Grounding on the logic of a well-recognized model, named MAXBAND, this study presents a signal optimization model, customized for the unique geometric features of Superstreet, which employs a multi-objective programming method to concurrently maximize the progression bandwidth and minimize delay experienced by minor road drivers.

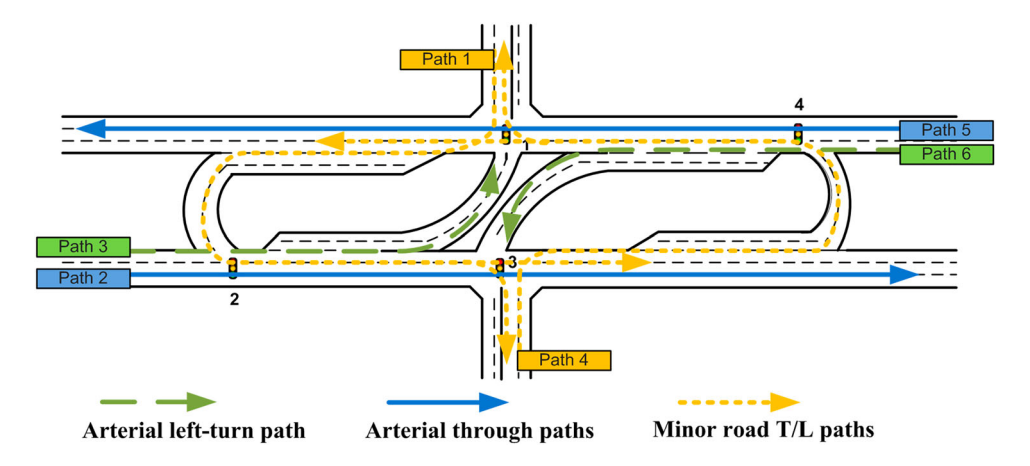


**Figure 1.** Paths illustration for a superstreet as a corridor segment.

In summary, the novel contributions of this paper are summarized as follows: (1) designed a two-stage modeling framework that can concurrently optimize signal plan, phase sequence, and offset of each sub-intersection at Superstreet so as to best utilize its capacity; (2) developed a multi-path progression model that can coordinate both heavy left-turn and through movements between main intersection and Uturn crossovers (as shown in Figure 1); (3) formulated the both internal and external queue constraints to prevent the potential queue spillover between closely-spaced subintersections; and (4) minimized the delays experienced by drivers from the minor approach and integrated such constraint into the Mixed-Integer-Linear-Programming (MILP) model.

#### 2. Literature review and research issues

Despite the short of the signal optimization methods for a Superstreet, a large body of studies for developing the best signal plan for conventional intersections are available in the literature. Since a Superstreet includes three sub-intersections, its signal design shall include optimizations at both intersection and arterial levels. For intersection signal optimization, existing studies in the literature have adopted various objective functions such as delay minimization, capacity maximization, PI (performance index) minimization, etc. In terms of formulating the traffic streams, one can category those models into two groups: group-based optimization and lane-based optimization. The first group (Allsop 1992; Heydecker 1992; Heydecker and Dudgeon 1987; Improta and Cantarella 1984; Tully 1976; Wong 1996; Gartner and Stamatiadis 2004) treats traffic movements within lane groups as units for optimization while the second group (Wong and Wong 2003) consider the variation of traffic distribution among different lanes.

Regarding the signal optimization at the arterial level, one may category those existing studies into the following two distinct types: minimizing the total delay or maximizing throughput. Most of those in the first category focused mainly on minimizing the total delay for intersections within the control boundaries, where TRANSYT family (Robertson 1969; Wallace et al. 1988), a simulation-based program, is one of the most commonly adopted tools by the traffic control community. Aiming for the same control objective, many researchers continued to develop the optimal signal plan with different mathematical algorithms. For example, to find the optimal solution for coordinated traffic signal timing plans along the arterial, Hadi and Wallace (1993) and Park, Messer, and Urbanik (1999) applied a genetic algorithm while Lo (1999, 2001) employed a cell-transmission model to investigate gueue dissipation and kinematic waves at signalized intersections. Similar researches that are aiming at minimizing various delays can also be found (Yun and Park 2006; Stevanovic, Martin, and Stevanovic 2007; Liu and Chang 2011). Studies that are more recent also attempted to respond to time-varying traffic flow with adaptive control (Keyvan-Ekbatani et al. 2012, 2013; Aboudolas and Geroliminis 2013; Christofa, Ampountolas, and Skabardonis 2016).

The focus of signal models in the second category is to synchronize offsets over successive intersections along an arterial so as to facilitate its progression movement. Little, Martin B, and Morgan J (1966) first presented a mixed-integer linear program model to optimize the offsets between intersections along an arterial to maximize the progression bands under the given cycle length. Based on this effort, Litter, Kelson, and Gartner (1981) further developed a model, called 'MAXBAND,' to generate the optimal offsets for maximizing the weighted bandwidths. Along the same line, Chang et al. (1988) presented MAXBND-86 to address the design of a left-turn phase sequence to optimize the arterial signal progression. Ground on the core logic of MAXBAND, Gartner et al. (1991) presented an optimization model (called 'MULTIBAND') for arterial progression that could generate an optimally weighted bandwidth for the arterial experiencing different traffic volumes in their links. Based on this approach, Stamatiadis and Gartner (1996) further developed an enhanced version, called 'MULTIBAND-96,' for multi-arterial traffic networks. Along the same line, some researchers formulate the problem to solve for optimal offsets with varying traffic volumes or phase sequences (Gartner and Stamatiadis 2002; Zhang et al. 2015). To address the application for such a model in practice, Tian and Urbanik (2007) developed a partition technique to decompose a network, and to facilitate the progression in the more important direction. Li (2014) presented a robust signal optimization method to account for uncertainty in the progression time. To contend with the need of synchronizing heavying turning flows along arterials, Yang, Cheng, and Chang (2015) developed three progression models to provide progression flows for identifying critical paths along an arterial based on the preliminary O-D flow estimates. Such a progression design logic has also been applied to design the signal plans for other unconventional intersections, like Diverging Diamond Intersection (Yang, Chang, and Rahwanji 2014).

Despite the promising development in signal control for conventional intersections, those methodologies may not be applicable to a typical Superstreet design due to its unique geometric characteristics. More specifically, as shown in Figure 1, the minor road drivers should pass through three sub-intersections successively to pursue their original direction. If the signals are not properly coordinated, they may experience excessive delays and consequently impair the intersection's overall performance. In addition, due to the heavy left-turning flows from the major approaches, one shall equally account for the left-turn and through movements (see Figure 1) in the design of signal progression. Failing to do so may lead to the potential queue spillback at those short left-turn bays and consequently reduce the Superstreet's capacity.

#### 3. Signal control algorithm

This study proposes a two-stage signal optimization model that intends to concurrently address the aforementioned key issues. The phase sequence for each sub-intersection is presented in Figure 2 and the index of all sub-intersections are shown in Figure 4.

Recognizing that a better design of both the cycle length and the offsets can impact a Superstreet's overall performance, the proposed signal optimization model comprises two stages. Stage 1 selects the best common cycle length for all sub intersections, and Stage 2 determines the offsets to achieve the signal progression and also to minimize the waiting time of drivers from the minor road. Figure 3 shows the iterative procedures between Stage 1 and Stage 2, where the process will be terminated if the change in the cycle length between two successive iterations is less than one second.

For the convenience of discussion, Table 1 summarizes the key notations for all model variables used thereafter.

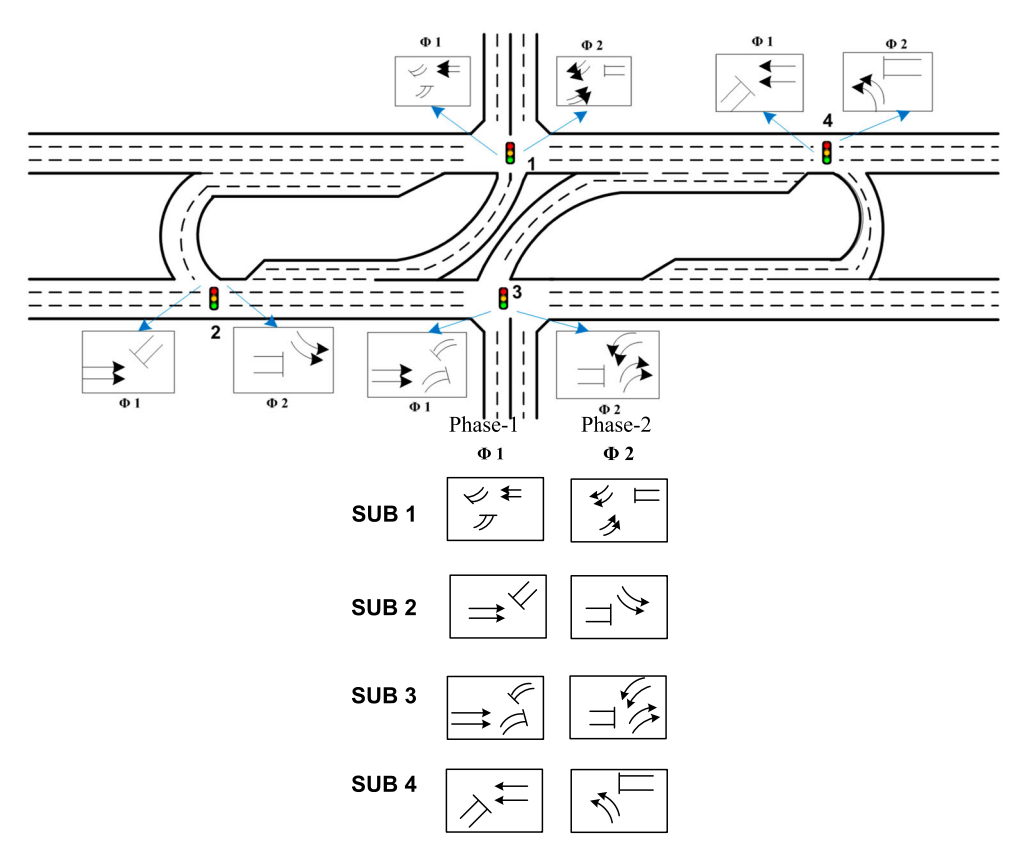
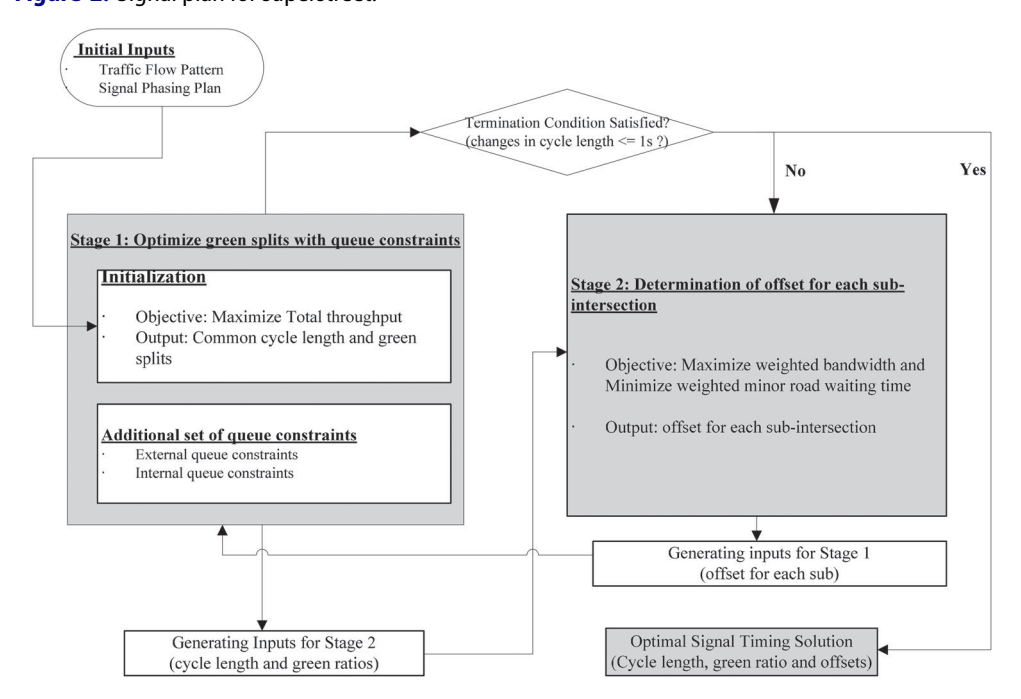


Figure 2. Signal plan for superstreet.



**Figure 3.** General algorithm of the proposed two-stage signal optimization.



**Table 1.** Notation for key variables/parameters.

Notation	Description					
Sets						
$I = \{1, 2, 3, 4\}$	Set of sub-intersections. 1 denotes the northern sub-intersection; 2 denotes the western one; 3 denotes the southern while 4 denotes the eastern one.					
$P = \{1, 2, 3, 4, 5, 6\}$	Set of paths					
$J = \{1, 2, \dots, 10\}$	Signal controlled movements group among entire superstreet, illustrated in Figure 4, where (2,3) and (7,8) belong to the same group.					
$K = \{1, 4\}$	Set of paths from minor roads					
Variables						
$\mu_i$	Multiplier to traffic volume at intersection <i>i</i> , representing ratio between actual capacity and the volume					
C	Common cycle length for all sub-intersections					
$\phi_{ij}$	Duration of green time for movement j at intersection i (proportional to cycle length)					
$\theta_i$	Offset of intersection i					
W <sub>ip</sub>	Time between the start of a cycle and the start of the band for path $p$ at intersection $i$					
$b_p$	Bandwidth for path <i>p</i>					
n <sub>ip</sub>	Integer indicator for cycle length; 0, 1, 2, , <i>n</i>					
$X_1, X_2, X_3$	Binary variables indicating green phase when $= 1$ ; o.w. indicating red phase					
ξ	The reciprocal of cycle length					
$T_{ik}$	The (waiting time/cycle length) ratio for path k vehicle at intersection i					
Parameters						
$\sigma_p$	Set of intersections passed by path-flow p					
S	Saturation flow rate (per lane)					
$t_I$	Lost time for each movement in seconds					
$\eta_p$	Weighting factor for path <i>p</i>					
$C_{\min}$	Minimum cycle length in real application					
$C_{max}$	Maximum cycle length in real application					
$g_{min}$	Minimum green time for one movement					
$g_{max}$	Maximum green time for one movement					
$t_{i,i+1}$	Travel time from sub-intersection $i$ to $i + 1$ .					
q <sub>ij</sub>	Traffic arrival rate for movement <i>j</i> at intersection <i>i</i> (per lane)					
$L_j$	Maximum queue length for external movements (in this case, $j = 2, 5, 7, 10$ )					
$lpha_{ij}$	Lane use factor for movement <i>j</i> at intersection <i>i</i>					
λ	Multiplier to total travel time for paths from minor road					

#### 4. Model development

#### 4.1. Initialization of stage 1 solution

The initialization step is to generate the initial signal plan that includes the common cycle length and the green splits for each sub intersection. The index for all traffic movements is denoted in Figure 4.

Since superstreets are often implemented when the major arterial flows are significantly larger than minor street flows, a control objective such as delay minimization may sacrifice the operational benefits of traffic on minor streets while throughput maximization becomes a better option. To formulate the problem with Linear Programming technique, this study adopts a variable to represent the intersection capacity. As reported in the literature (Yagar 1975; Xuan, Daganzo, and Cassidy 2011), a well-designed signal plan needs to achieve the capacity maximization under the given intersection geometry. Based on the assumption that traffic demand matrix can be multiplied with a common multiplier to represent the maximum amount of the increased volume that would still allow the intersection to perform reasonably well (Wong 1996; Wong and Wong 2003), the objective function at the

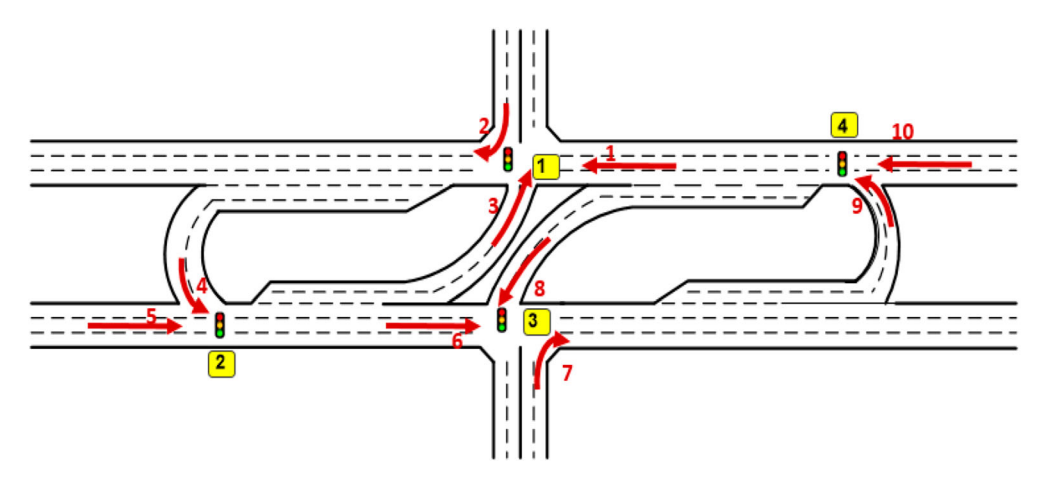


Figure 4. Illustration of index for each movement among a typical superstreet.

initialization stage is to search for the maximal multiplier and be expressed as follows:

$$\mathsf{Max}\left(\sum_{i\in I}\mu_i\right) \tag{1}$$

By maximizing the summation of  $\mu_i$  for all sub-intersections, the overall intersection throughput can be reasonably optimized. Note that the corresponding sub-intersection intersection is at the over-saturated traffic state if the generated  $\mu_{\text{max}}$  is less than 1.

Given the traffic demand pattern at each intersection, it is nature that the following constraint be specified to ensure that the degree of saturation at each movement is below the acceptable limit:

$$\mu_i \alpha_i q_{ii} \le s(\phi_{ii} - \xi \times t_l) \quad \forall i, j \tag{2}$$

For any selected common cycle length, it should fall within the range of acceptable limits:

$$\frac{1}{C_{\text{max}}} \le \xi \le \frac{1}{C_{\text{min}}} \tag{3}$$

The green ratio for each movement group should also be subjected to the following constraint:

$$\xi \times q_{\min} < \phi_{ii} < q_{\max} \times \xi \tag{4}$$

Since each sub-intersection has one signal controller, its sum of all g/c ratios should be equal to 1:

$$\phi_{ij_1} + \phi_{ij_2} = 1$$
  $j_1 j_2 \in J \text{ and } j_1 \neq j_2$  (5)

Notably, using throughput maximization as objective will result in maximum cycle length and potentially larger average delay. To overcome this issue, this study implements

Webster's formula to determine the reasonable range of cycle length:

$$C = \frac{1.5 \times L + 5}{1.0 - \Psi/s} \tag{6}$$

$$C_{\text{max}} = C + \Delta C \tag{7}$$

$$C_{\min} = C - \Delta C \tag{8}$$

where L is the total lost per cycle;  $\Psi$  is the critical lane volume (CLV) at the most congested intersection; s is the saturation flow rate;  $\Delta C$  is the maximum allowed cycle length variations (e.g., 10 s).

In brief, one can present the formulations for the initialization stage as follows:

Maximize 
$$\sum_{i \in I} \mu_i$$
 s.t. Equations (2)  $-$  (8)

#### 4.2. Stage 2 - Computing the offsets for each sun-intersection

Stage 2 proposes a multi-objective mixed integer linear programming model, which aims to maximize the weighted bandwidth and concurrently minimize the delay experienced by the minor road drivers. Figure 1 (in page 6) shows the critical paths among a signalized Superstreet, where paths 1, 4 denote the through and left-turn movements from the minor roads; paths 2, 5 are the arterial's through and right-turn movements and paths 3, 6 represent the arterial's left-turning flows.

In order to achieve the signal progression and minimal waiting time for the minor road drivers, one should formulate the control objective as follows:

$$\operatorname{Max}\left(\sum_{p\in P}\eta_p b_p - f_k \sum_{k\in K} T_{ik}\right) \tag{9}$$

Note that by adjusting  $\eta_p$  and  $f_k$ , one can set one of these two goals to a higher priority. In this case, the bandwidth maximization is set as the first priority since the main benefit of such a design is to provide uninterrupted arterial flows.

As there are only two phases for each sub-intersection, the impact of the phase sequence on the entire Superstreet's operational performance is negligible. In addition, the constraints (as shown in Equations (7)–(10)) should be satisfied for the weighted bandwidth maximization. Figure 5 presents the graphical illustration of each term.

For each direction, as  $\theta_i$  denotes the offset at sub-intersection i, its interference constraints which ensure the sum of the bandwidths and  $w_{ip}$  should not exceed the total green time (see Figure 5) are listed below:

$$0 < w_{in} + b_n < q_{in} \tag{10}$$

$$w_{ip}, \quad b_p \ge 0 \tag{11}$$

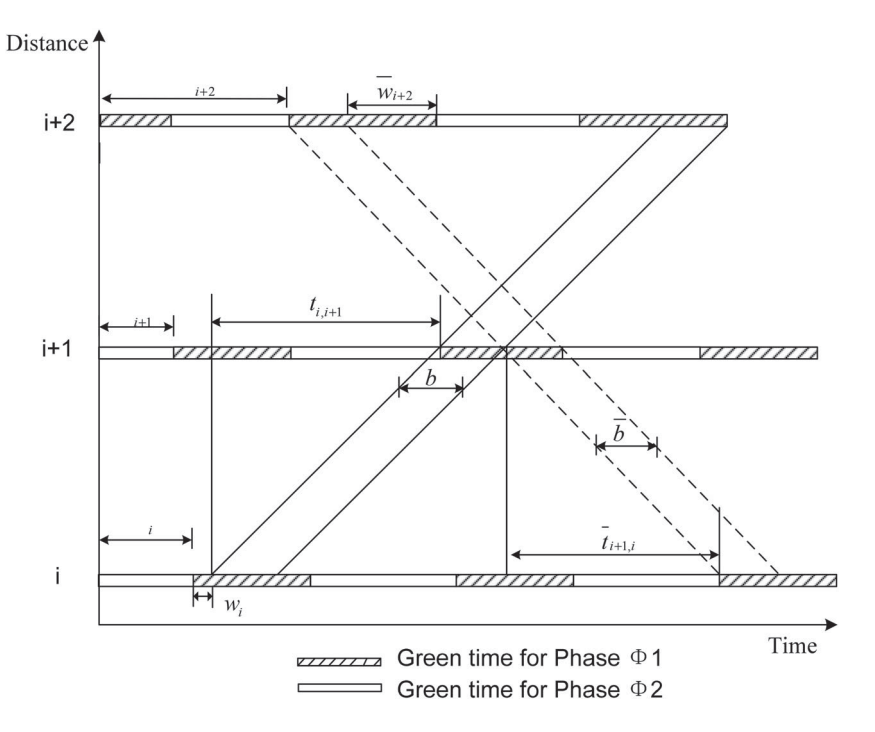


Figure 5. Time-space diagram for MAXBAND.

As in most progression formulations, the loop integer constraint for each path can be expressed as follows:

$$\theta_{i} + r_{ip} + w_{ip} + t_{i,i+1} + n_{ip}C \ge \theta_{i+1} + r_{i+1,p} + w_{i+1p} + n_{i+1p}C \quad \forall p \in P; \quad \forall i \in \sigma_{p} \quad (12)$$

$$\theta_i + r_{ip} + w_{ip} + t_{i,i+1} + n_{ip}C \le \theta_{i+1} + r_{i+1p} + w_{i+1p} + n_{i+1p}C \quad \forall p \in P; \quad \forall i \in \sigma_p$$
 (13)

Note that constraints presented above are based on the core notion of MAXBAND (Litter, Kelson, and Gartner 1981), which is used to provide the progression band for all critical paths within a Superstreet. However, one needs to specify proper constraints to avoid the excessive waiting time experienced by the minor road drivers due to the signal control. Taking path 1 as an example, the minor road drivers in this path have to pass three successive sub-intersections, including sub-intersections 1, 2 and 3. Note that it is not desirable for a vehicle to wait at every red phases at all the sub-intersections. The proposed waiting time constraints are formulated to describe the total waiting time of a vehicle during the entire red phase at the first sub intersection, because the red phase duration at sub-intersection 1 usually is the main contributor to the total waiting time over all sub-intersections. The waiting time ratio (denoted as  $T_{11}$ ) for such vehicles at sub-intersection 1 can be expressed as follows:

$$T_{11} \ge \phi_{11}$$
 (14)

where  $\phi_{11}$  denotes the ratio of the red phase over the cycle length at sub-1, which is also the green time for movement 1. After passing sub-intersection 1, whether or not such vehicles

will hit the red phase at sub-intersection 2 can be represented with a binary variable  $x_{11}$ , where M is a sufficiently large positive number:

$$x_{11} \ge \frac{\theta_2 + \phi_{25} - \theta_1 - \phi_{11} - t_{12} * \xi}{M} \tag{15}$$

$$x_{11} \le \frac{\theta_2 + \phi_{25} - \theta_1 - \phi_{11} - t_{12} * \xi}{M} + 1 \tag{16}$$

Note that since  $t_{12}$  is the travel time (in seconds) from sub-intersections 1–2, it can be converted into a time ratio by multiplying  $\xi$ .

As presented in Figure 6(b), if the signal plans for sub-intersections 1 and 2 follow the graphical presentation, then the leading vehicle departing right after the end of  $\phi_{11}$  will hit the red phase at the downstream sub-intersection 2 (The green phase for vehicles in movement 5, denoted as  $\phi_{25}$ ). On the other hand, if vehicles from sub-intersection 1 encounter the green phase at sub-intersection 2, as shown in Figure 6(a), then  $x_{11}$  will be set to 0.

As shown in Equation (14), if the incoming vehicles in path 1 hit the green phase at the downstream signal, where  $x_{11} = 1$ , then the following relaxation will exist.

$$\theta_2 + \phi_{25} - \theta_1 - \phi_{11} - t_{12} * \xi \ge 0; \tag{17}$$

If  $x_{11}$  equals 1, the waiting time ratio (the waiting time/cycle length) for path 1 vehicles at sub-intersection 2 (represented as  $T_{21}$ ), which are denoted in Figure 6(b), can be expressed as follows:

$$T_{21} \ge (\theta_2 + \phi_5 - \theta_1 - \phi_1 - t_{12} * \xi) - (1 - x_{11})M; \quad T_{21} \ge 0$$
 (18)

On contrast, if  $x_{11} = 0$ , this constraint will be relaxed since  $T_{21}$  is strictly non-negative.

Following the same logic, the maximal waiting time experienced by vehicles in path 1 due to a signal control can be denoted as the sum of  $T_{11}$ ,  $T_{21}$ ,  $T_{31}$  (as shown in Figure 7). Following the same logic, one can express  $T_{21}$ ,  $T_{11}$  and  $T_{31}$  with Equations (16)–(19):

$$x_{21} \ge \frac{\theta_2 + \phi_{25} + t_{23} * \xi - \theta_3 - \phi_{36}}{M} \tag{19}$$

$$x_{21} \le \frac{\theta_2 + \phi_{25} + t_{23} * \xi - \theta_3 - \phi_{36}}{M} + 1 \tag{20}$$

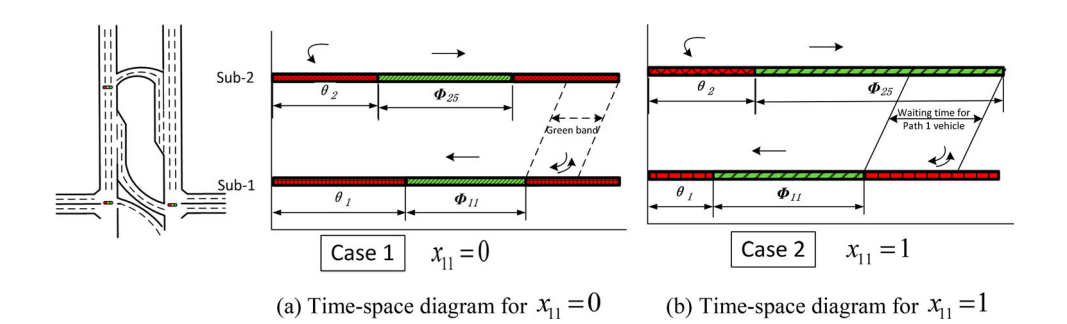


**Figure 6.** Graphical illustration of binary variable.

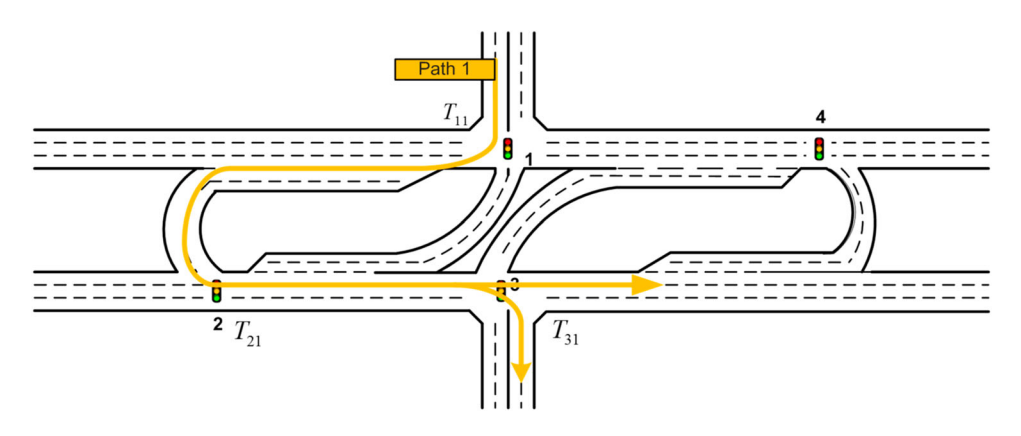


Figure 7. Route for vehicles from path-1.

$$T_{31} \ge (1 - \theta_2 - \phi_{25} - t_{23} * \xi + \theta_3) - (1 - x_{11})M - (1 - x_{21})M$$
 (21)

$$T_{31} \ge (1 - \theta_1 - \phi_{11} - t_{12} * \xi - t_{23} * \xi + \theta_3) - x_{11}M - (1 - x_{21})M; \quad T_{11}, T_{21}, T_{31} \ge 0$$
 (22)

The sum of the waiting time ratios at all sub-intersections should be less than the following preset threshold:

$$T_{11} + T_{21} + T_{31} < \lambda \xi * (t_{12} + t_{23})$$
 (23)

where  $\lambda$  is the multiplier for the sum of travel times from intersections 1–2 and from 2 to 3. The sum of  $t_{12}$ ,  $t_{23}$  is the travel time from sub-intersections 1–3 without a signal control. When multiplied by  $\xi$ , it can be further converted into a ratio, the preset upper bound for the total waiting time ratio experienced by vehicles in path 1.

In brief, one can summarize all formulations in stage-2 as follows:

$$\mathsf{Maximize}(\sum_{p \in P} \eta_p b_p - f_k \sum_{k \in K} T_{ik})$$

s.t.

for all critical paths : Equations (10) - (14)

for minor road paths: Equations (14) - (23)

#### 4.3. Stage 1 – optimization of green splits with queue constraints

With the algorithm summarized in Figure 3 (see page 8), one can get a set of offsets for each sub-intersection based on the common cycle length generated at the initialization step. Note that the initialization does not account for the potential queue impacts on the traffic progression. Hence, aside from keeping all such constraints and the objective function at the initialization, Stage 2 adds a set of queue constraints to prevent the formation of traffic spillback. Figure 8 shows the spatial distribution of all potential queues among a Superstreet.

#### 4.3.1. External queues: Q2, Q5, Q7, Q10

Figure 9 illustrates the external queue formation process, which consists of two components: the vehicle accumulated during the red phase and the residual queue during

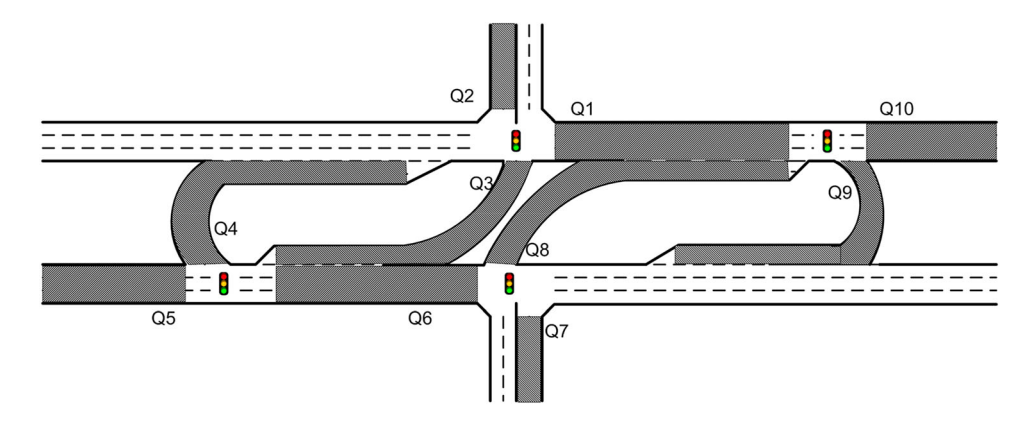


Figure 8. Spatial queue distribution among a superstreet.

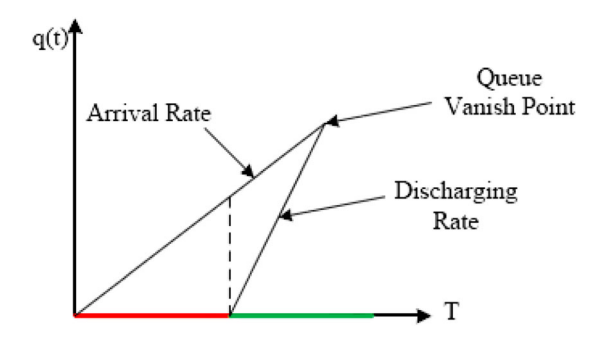


Figure 9. Queue formation process.

the initial green time. To prevent queue spillback, the maximum allowable queue cannot exceed the link length. Note that the vehicle arrival is assumed to follow uniform distribution and no residual queue exist among a Superstreet.

One can then derive the following expression,

$$L_j = \frac{(1 - \phi_{ij} + t_l * \xi) * \alpha_{ij} q_{ij} * s}{(s - \alpha_{ij} q_{ij}) \xi}$$
(24)

where  $L_j$  denotes the link length for queue j, while  $j \in J$  is the set of all potential queues. The following queue length constraints are specified to prevent external-queue spillback:

$$(1 - \phi_{12} + t_1 * \xi)\alpha_{12}q_{12}s < L_2(s - \alpha_{12}q_{12})\xi \tag{25}$$

$$(1 - \phi_{25} + t_1 * \xi)\alpha_{25}q_{25}s \le L_5(s - \alpha_{25}q_{25})\xi \tag{26}$$

$$(1 - \phi_{37} + t_1 * \xi)\alpha_{37}q_{37}s < L_7(s - \alpha_{37}q_{37})\xi \tag{27}$$

$$(1 - \phi_{410} + t_l * \xi)\alpha_{410}q_{410}s < L_{10}(s - \alpha_{410}q_{410})\xi$$
 (28)

#### 4.3.2. Internal queues: Q1, Q6, Q3, Q8, Q4, Q9

Note there are initial offsets for all sub-intersections produced in stage-1 and the set of binary parameters  $(f_1, f_3, f_4, f_6, f_8, \text{ and } f_9)$  can then be determined accordingly. The additional notations for the set of internal queue constraints are shown in Table 2.

<b>Table 2.</b> Additional	variable	notation	for	the	set	of	queue	con-
straints.								

Notation	Description				
L <sub>j</sub>	Link length for certain movement j				
$f_1$	Binary parameter; ( $=$ 1, if $\theta_1 \ge \theta_4 + t_{41} * \xi$ ; o.w $=$ 0)				
$f_3$	Binary parameter; ( = 1, if $\theta_1 \ge \theta_2 + t_{21} * \xi$ ; o.w = 0)				
$f_4$	Binary parameter; ( = 1, if $\theta_1 \ge \theta_2 - t_{12} * \xi$ ; o.w = 0)				
$f_6$	Binary parameter; ( = 1, if $\theta_3 \ge \theta_2 + t_{23} * \xi$ ; o.w = 0)				
f <sub>8</sub>	Binary parameter; ( = 1, if $\theta_3 \le \theta_4 + t_{43} * \xi$ ; o.w = 0)				
f <sub>9</sub>	Binary parameter; ( = 1, if $\theta_3 \ge \theta_4 - t_{34} * \xi$ ; o.w = 0)				
<i>y</i> <sub>4</sub>	Binary variable; ( = 1, if $\theta_1 + \phi_{11} \le \theta_2 + \phi_{25} - t_{12} * \xi$ ; o.w = 0)				
<b>y</b> 9	Binary variable; ( = 1, if $\theta_3 + \phi_{36} \le \theta_4 + \phi_{410} - t_{34} * \xi$ ; o.w = 0)				
<i>y</i> <sub>6</sub>	Binary variable; ( $=$ 1, if $ heta_3 + \phi_{36} - t_{23} * \xi \le \theta_2 + \phi_{25}$ ; o.w $=$ 0)				
<i>y</i> <sub>1</sub>	Binary variable; ( $=$ 1, if $\theta_1 + \phi_{11} - t_{41} * \xi \le \theta_4 + \phi_{410}$ ; o.w $=$ 0)				
<i>y</i> <sub>3</sub>	Binary variable; ( = 1, if $\theta_2 + \phi_{25} \le \theta_1 + \phi_{11} - t_{21} * \xi$ ; o.w = 0)				
<i>y</i> <sub>8</sub>	Binary variable; ( $=$ 1, if $\theta_4 + \phi_{410} \le \theta_3 + \phi_{36} - t_{43} * \xi$ ; o.w $=$ 0)				
$Q_{j}^{\prime},Q_{j}^{\prime\prime}$	Partial internal queues for movement <i>j</i>				

The set of internal queues can further be categorized into the following three types:

- Type-1 internal U-turn queue: Q4 and Q9 (U-turn crossover queue);
- Type-2 internal left-turn queue: Q3 and Q8 (main left-turn queue on arterial);
- Type-3 internal through queue: Q1 and Q6 (main through queue on arterial).

4.3.2.1. Type-1 internal queue: Q4 and Q9 (U-turn crossover queue). These types of queues are contributed by the left-turn and through vehicles from the minor streets. If those incoming vehicles encounter a red phase at the downstream U-turn crossover, the queue will start to accumulate. To formulate such relations, let the binary variable,  $y_4$ , represent the downstream signal phase during the arrival of upstream vehicles. Taking Q4 as an example, it may be formed over two intervals. The queue lengths accumulated during these two time intervals are denoted as  $Q_4$  and  $Q_4$ , respectively.

As presented in Figure 10, the status  $y_4 = 1$  indicates that the incoming vehicle hits the red phase at the downstream sub-intersection 2, while  $y_4 = 0$  stands for a green phase at sub-intersection 2. The mathematical expression for  $y_4$  can be expressed as follows:

$$y_4 \ge \frac{\theta_2 + \phi_{25} - t_{12} * \xi - \theta_1 - \phi_{11}}{M} \tag{29}$$

$$y_4 \le \frac{\theta_2 + \phi_{25} - t_{12} * \xi - \theta_1 - \phi_{11}}{M} + 1 \tag{30}$$

Note that since all these offsets and phase durations are expressed in time ratios, the travel time  $t_{12}$  is multiplied by  $\xi$  as to be transferred in ratios. Hence, the maximal length of  $Q_4$  during such a time period can be formulated as follows:

$$Q_4' \ge (\theta_2 + \phi_{25} - \theta_1 - \phi_{11} - t_{12} * \xi)\alpha_{24}q_2^{LT} - (1 - y_4)M; \quad Q_4' \ge 0$$
 (31)

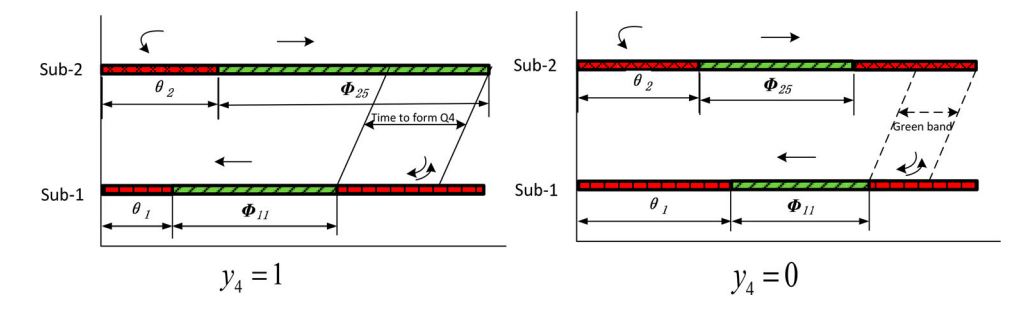


**Figure 10.** Graphical illustration of binary variable  $y_4$ .

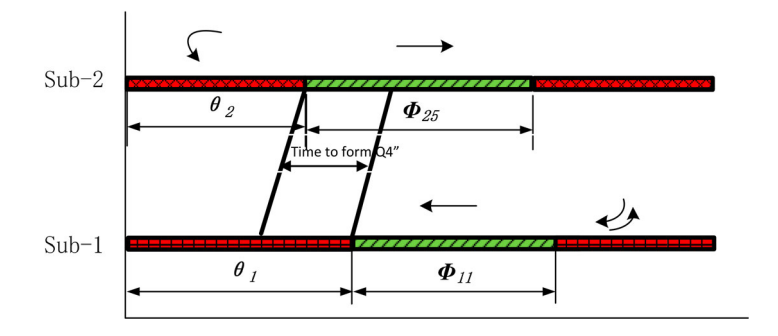


**Figure 11.** Graphical illustration for binary parameter  $f_4 = 1$ .

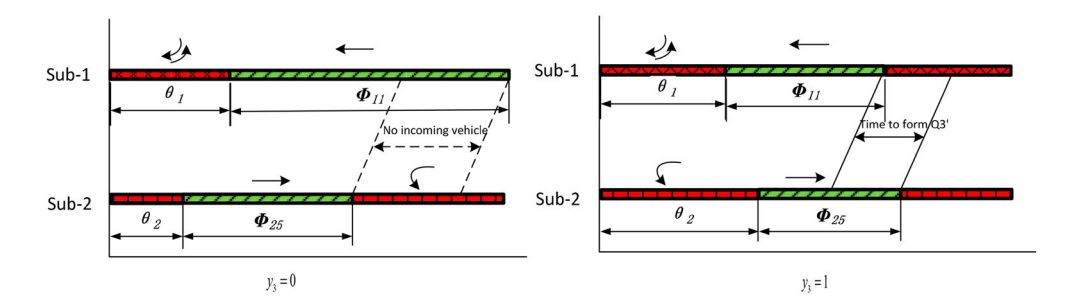


**Figure 12.** Graphical illustration for binary variable  $y_3$ .

If  $y_4 = 0$ , this constraint will be relaxed since  $Q_4$  is strictly non-negative. Except for the time to form  $Q_4$ , the other possible time duration to form  $Q_4$  is denoted in Figures 5–13. A binary parameter  $f_4$  is introduced as follows:

$$f_4 = \begin{cases} 1 & \text{if } \theta_2 < \theta_1 + t_{12} * \xi; \\ 0 & o.w \end{cases}$$
 (32)

Note that  $f_4$  is the indicator to indicate whether or not the incoming flows will hit the red phase at sub-2 as shown in Figure 11.

The queue length,  $Q_4''$ , accumulated during such a time period (as denoted in Figure 11) can be expressed with Equations (5)–(30). Note that  $q_2^{LT}$  is the demand for left-turn and

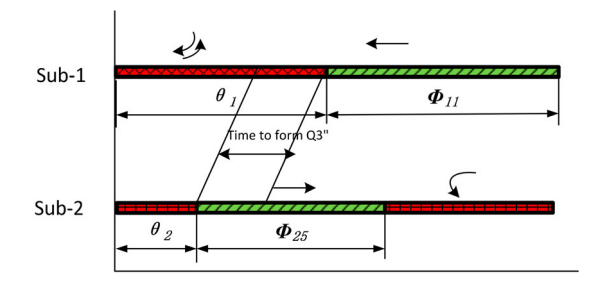


**Figure 13.** Graphical notation for  $f_3 = 1$ .

through vehicles departing from Q2.

$$Q_4'' = \alpha_4 q_2^{LT} f_4(\theta_1 - \theta_2 + t_{12} * \xi)$$
(33)

So the maximum queue length for link 4 during each cycle can be expressed as the sum of the vehicles accumulated during these two time durations.

$$Q_4' + Q_4'' \le \xi L_4 \tag{34}$$

The maximum length of Q4 cannot exceed the link length, denoted as  $L_4$ . The same methodology can be applied to derive a queue constraint for Q9.

4.3.2.2. Type-2 internal queue: Q3 and Q8 (main left-turn queue). Vehicles forming this type of internal queues are the departures from Q5 and Q10. Similar to the methodology to obtain Q4, a set of binary parameters and variables should be defined first to denote the signal phase at the downstream sub-intersection. Likewise, a binary variable  $y_3$  is set to 1 if the departures from Q5 encounter the red phase at sub-intersection 1; otherwise, it will be equal to 0.

$$y_3 \ge \frac{\theta_2 + \phi_{25} + t_{21} * \xi - \theta_1 - \phi_{11}}{M} \tag{35}$$

$$y_3 \le \frac{\theta_2 + \phi_{25} + t_{21} * \xi - \theta_1 - \phi_{11}}{M} + 1 \tag{36}$$

A graphical illustration for a definition of  $y_3$  is shown in Figure 12.

Thus, one can formulate a maximum length of  $Q_3$  during this time period as shown below:

$$Q_3' \ge (\theta_2 + \phi_{25} + t_{21} * \xi - \theta_1 - \phi_{11})\alpha_{13}q_5^L - (1 - y_3)M; \quad Q_3' \ge 0$$
 (37)

If  $y_3 = 0$ , this constraint (Equation (34)) will be relaxed since  $Q_3$  is strictly non-negative. Except for the time to form  $Q_3$ , the other possible time duration is denoted as  $Q_3$ " (as shown in Figure 13). A binary parameter,  $f_3$ , is introduced as follows:

$$f_3 = \begin{cases} 1 & \text{if } \theta_1 \ge \theta_2 + t_{21} * \xi \\ 0 & \text{o.w} \end{cases}$$
 (38)

The queues accumulated during that time period (i.e  $f_3 = 1$ ) can be shown below:

$$Q_3'' = \alpha_3 q_5^L * f_3(\theta_1 - t_{21} * \xi - \theta_2)$$
(39)

Hence, the maximum queue length in link 3 during each cycle can be expressed as the sum of the vehicles accumulated during these two possible durations (specified as  $Q_3$ ' and  $Q_3$ '', respectively) as follows:

$$Q_{3}' + Q_{3}'' \le \xi L_{3} \tag{40}$$

where  $q_5^L$  is the flow rate for left-turn vehicles from Q5. The maximum length of Q3 cannot exceed the link length  $L_3$ . The same methodology can be applied to derive the queue constraint for link 8.

**4.3.2.3.** Type-3 internal queue: Q1 and Q6 (Main Through queue). Different from the previous two types, there are two possible sources to contribute to this type of queue. Taking Q1 as an instance, both the departures from Q4 and Q5 can contribute to the formation of Q1. Let Equation (38)–(39) be used to define a binary variable  $y_1$ :

$$y_1 \ge \frac{\theta_4 + \phi_{410} + t_{41} * \xi - \theta_1 - \phi_{11}}{M} \tag{41}$$

$$y_1 \le \frac{\theta_4 + \phi_{410} + t_{41} * \xi - \theta_1 - \phi_{11}}{M} + 1 \tag{42}$$

Figure 14 shows a graphical illustration of  $y_1$  under two different states.

Thus the maximum length of  $Q_1'$  and  $Q_1''$  during such time interval can be formulated as follows:

$$Q_{1}' \geq (\theta_{4} + \phi_{410} - \theta_{1} - \phi_{11} + t_{41} * \xi)\alpha_{11}q_{10}^{T} - (1 - y_{1})M; \quad Q_{1}' \geq 0$$

$$(43)$$

$$Q_1'' \ge (1 - \theta_4 - \phi_{410} - t_{41} * \xi)\alpha_{11}q_9 - (1 - y_1)M; \quad Q_1' \ge 0$$
 (44)

If  $y_1 = 0$ , this constraint will be relaxed since  $Q_1'$ ,  $Q_1''$  are strictly non-negative. Note that the  $Q_1'$  and  $Q_1''$  denote the partial queues on link 1 formed by two different incoming flows

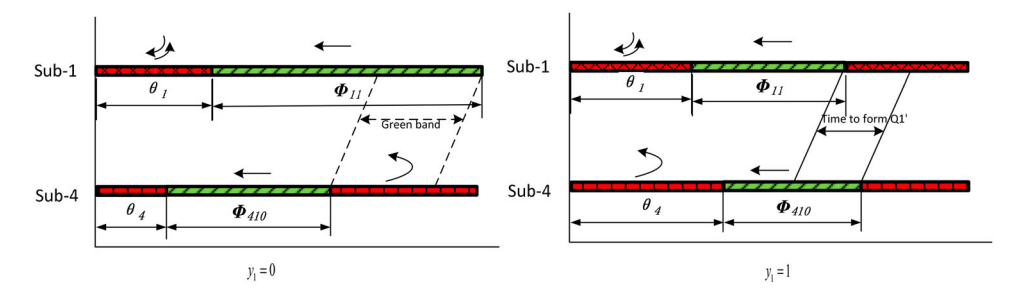


**Figure 14.** Graphical notation for  $y_1$ .

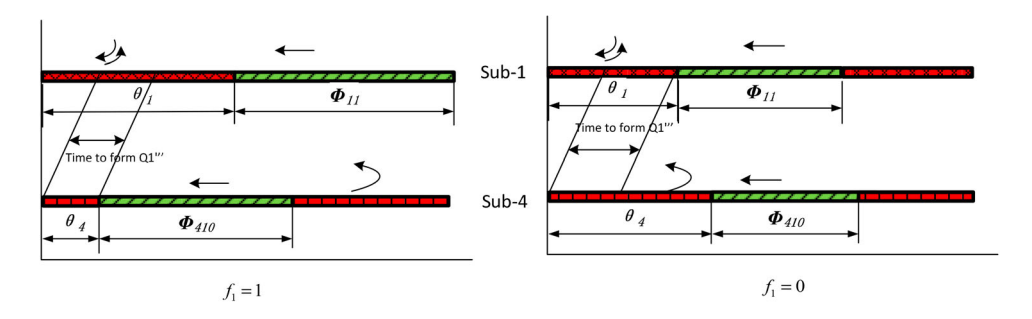


**Figure 15.** Graphical illustration for binary parameter  $f_1$ .

under the scenario that  $y_1 = 1$ . Except for the time to form  $Q_1'$  and  $Q_1''$ , the other possible time durations are denoted in Figure 15. To facilitate the presentation, one needs to further introduce a binary parameter  $f_1$ , where

$$f_1 = \begin{cases} 1 & \text{if } \theta_1 \ge \theta_4 + t_{41} * \xi \\ 0 & \text{o.w} \end{cases}$$
 (45)

$$Q_1^{"'} \ge f_1 * \theta_4 \alpha_{11} * q_{10}^T + (1 - f_1) * \alpha_{11} q_9 * \theta_1; \quad Q_1^{"'} \ge 0$$
 (46)

So the maximum length of queue on link 1 during each cycle can be expressed as the sum of the vehicles accumulated during those three possible time durations as shown below:

$$Q_1' + Q_1'' + Q_1''' \le \xi L_1 \tag{47}$$

where  $q_{10}^T$  is the demand for through vehicles departing from Q10, and  $q_9$  stands for departures from Q9. The maximum length of Q1 cannot exceed the link length  $L_1$ . The same methodology can be applied to derive Q6.

In brief, the Stage-1 formulations with queue constraints can be summarized as follows:

Maximize 
$$\sum_{i \in I} \mu_i$$

s.t.

general constraints : Equations (2) - (8)

for external queue : Equations (25) - (28)

for internal queue: Equations (29) - (47)

After running Stage 1, the new common cycle length will be taken as the input to re-run Stage 2. The results from Stage 2 will be set as a new input in Stage 1, and the iteration will go on until reaching the termination condition.

#### 5. Numerical examples

To evaluate the effectiveness of the proposed model, this study compares its performance with the signal plan produced by SYNCHRO 7.1. To further assess the necessity of the embedded queue constraints and the delays of minor-road vehicles, this study has

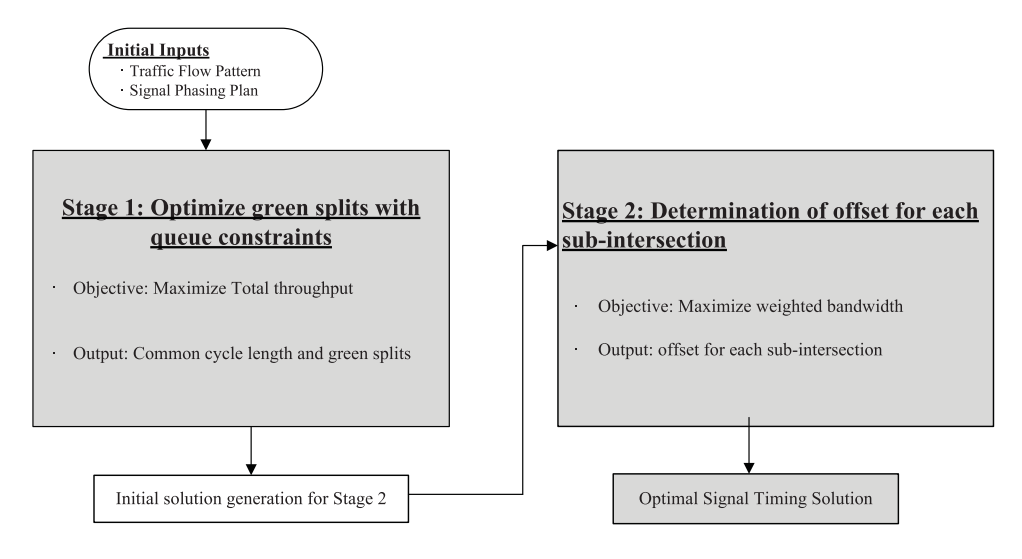


Figure 16. General algorithm of the base model.

also implemented the MAXBAND model for comparison. Since MAXBAND is only able to produce the offset between neighboring intersections, we have integrated it with the proposed stage-1 model which would generate green splits. The integrated model has named it as 'base model' as shown in Figure 16.

The numerical example is based on the field data collected from intersection MD 3 at Waugh Chapel Road in Maryland. The geometric layout and volume distribution of this intersection are shown in Figure 17(a,b), respectively.

The phase plan, phase sequence, signal plan, and coordination plan generated by the above three models are shown in Figure 18. Notably, the proposed model generates the smallest cycle length (67 s), while Synchro and the base model produce the cycle length

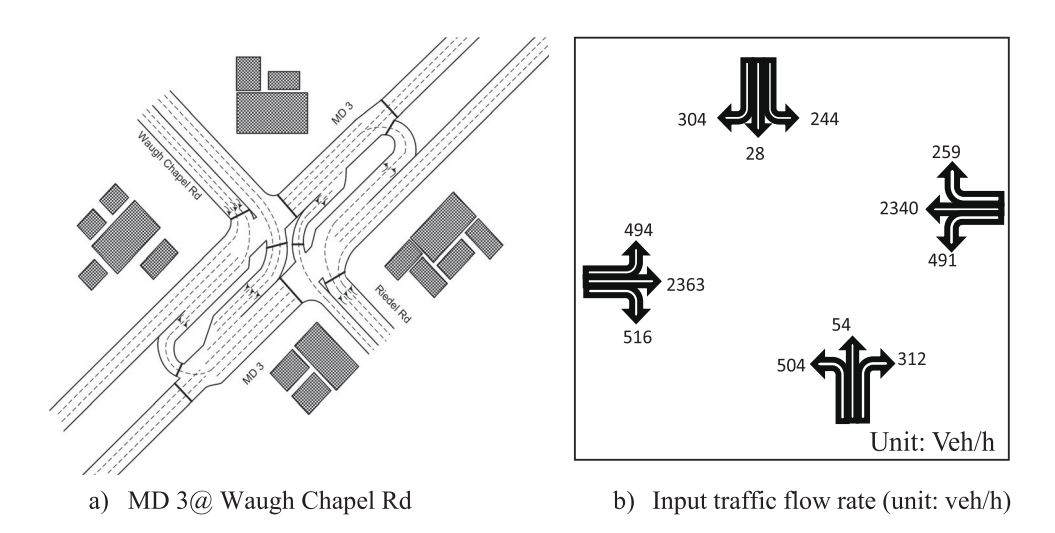


Figure 17. Target intersection geometry and input traffic flow rate.

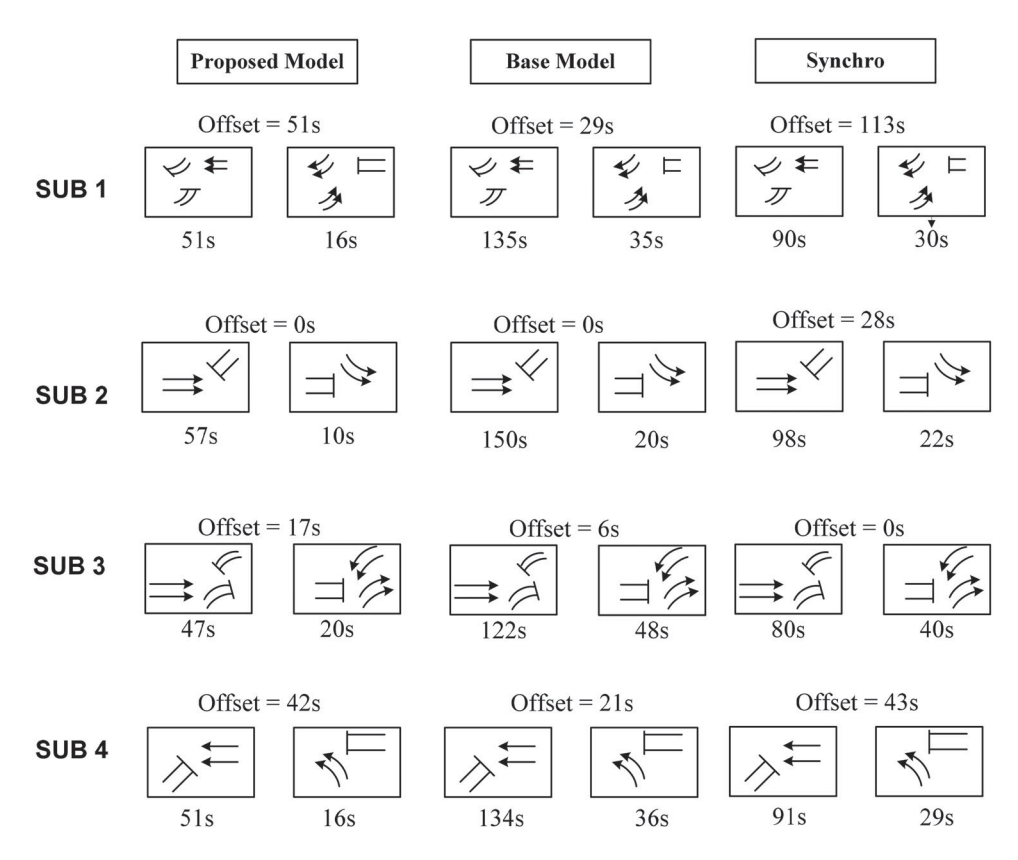


Figure 18. Optimal Green Splits and Offsets Produced by Different Models

120 and 170 s, respectively. This is due to the embedded queue constraints in the proposed model which function to prevent link queue spillback with a shorter common cycle length. Also, note that in the proposed model, the constraint for Q6 has been relaxed as its maximum queue exceeds its designed link length.

To further investigate the progression efficiency of the defined critical paths generated by the proposed model and the MAXBAND model, the resulting green bandwidths are presented in Figures 19 and 20, respectively. Due to the objective of maximizing the green band on the main arterial, the two paths for minor road drivers don't receive signal progression in both models.

Note that the offset for each sub-intersection has been listed on the right-hand side in the band diagram. As shown in Figures 19 and 20, one can observe that only the four paths along the arterial receive green bands, but not for the two minor road paths. This is consistent with the fact that the arterial's through and left-turn traffic volumes clearly receive a higher priority than those minor street flows.

To further assess the reliability of the evaluation results, this study has calibrated a Superstreet simulator to test whether this model can effectively prevent the formation of the queue spillbacks while achieving the predefined optimal conditions. To capture the flow variations in real-world traffic conditions, the analysis has conducted 30 simulation replications to perform the comparison studies. The maximal queue length from simulations on

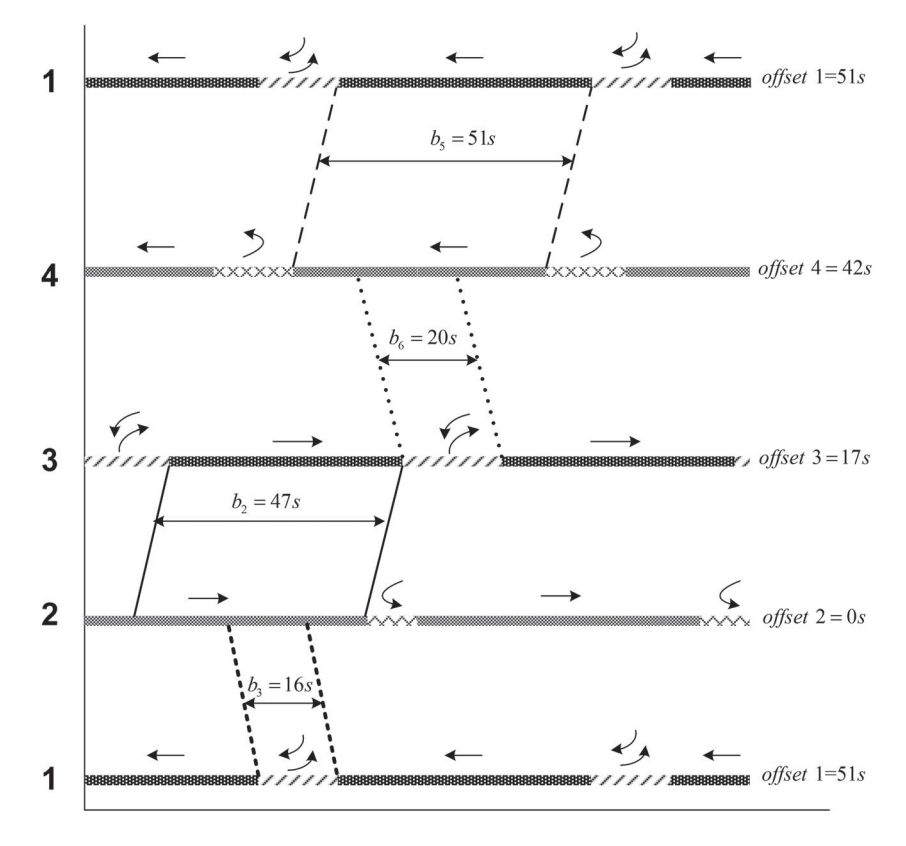


Figure 19. The green band solution obtained by the proposed model.

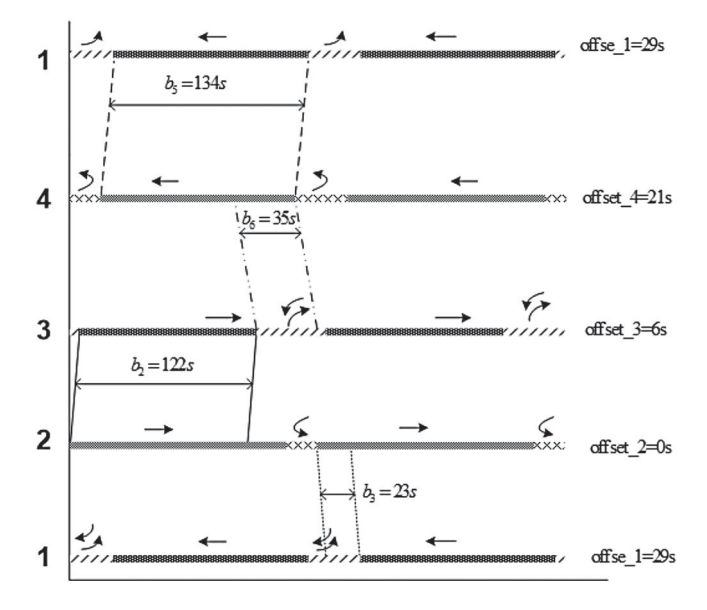


Figure 20. The green band solution obtained by the base model.

each critical link with different signal plans and the field measured link length are shown in Figure 20. It is noticeable that most simulated queues under the proposed model are much shorter than those under the base model and Synchro. Although most of those critical links are not under the risk of having queue spillback, Q7 under these three models has exhibited quite different patterns. The proposed model effectively limits the maximum queue length without exceeding the designed link length, while the other two models fail to prevent such

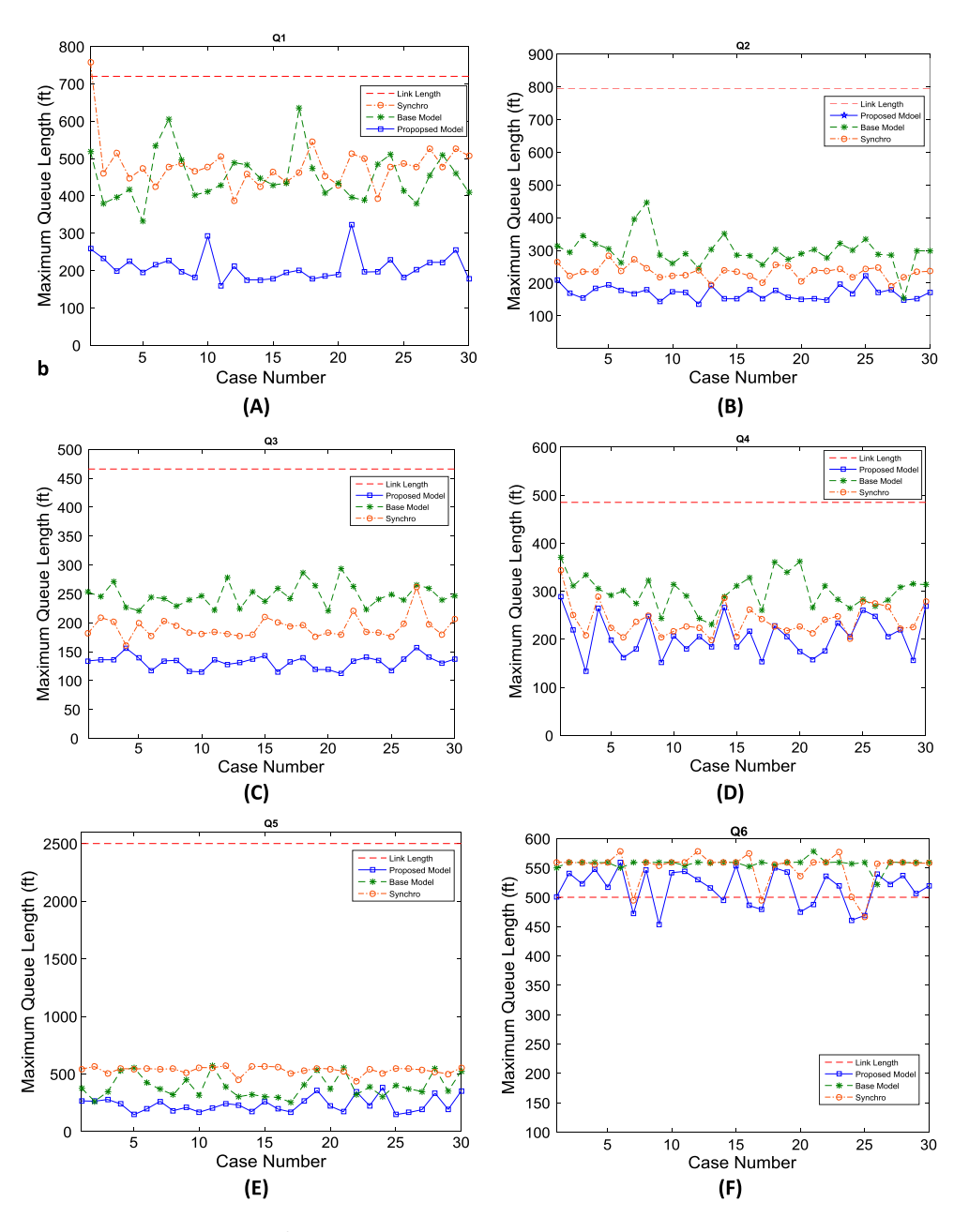


Figure 21. The distribution of all simulated maximum queue lengths under three signal plans.



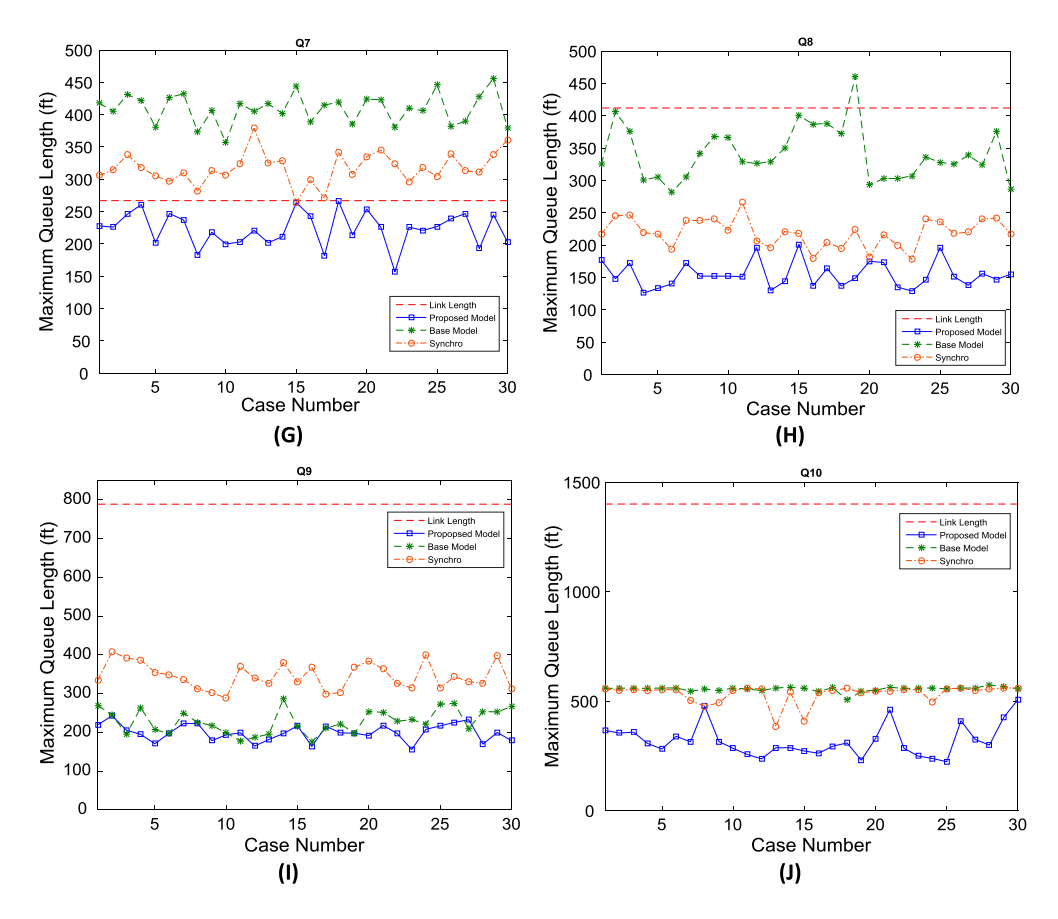


Figure 21. Continued.

blockages. The maximum queue length distribution of Q6 shows that all signal plans fail to prevent the formation of queue spillback.

Moreover, there is no evidence that the Synchro can outperform the base model due to the fact that it generates the longest maximum queues in some links (Q5, Q6 and Q9) than the other two models (as shown in Figure 20(E,I,F)).

The simulation results also show that the queue spillover on some critical links (e.g. Q6, and Q7) indeed occurs on the Superstreet, if designed with the longer cycle length as produced by the base model and Synchro. Such queue spillovers can result in several blockages on the left-turn bay and through lanes, and consequently increase the average delay over the entire intersection. The resulting average traffic delays over the entire Superstreet under three different signal plans are summarized in Figure 21. It is clear that the proposed model can produce the lowest average intersection delay among all cases.

Overall, the proposed model, as expected, can evidently provide effective signal progression for these critical paths under heavy arterial flows in a Superstreet. By comparing the network performance under three different signal plans, this study has selected the maximum queue length on each critical link and average intersection delay as MOEs. As shown in Figure 21, the proposed model generates the lowest average delay among all three models due to the embedded minimization of the minor road delay and the set of

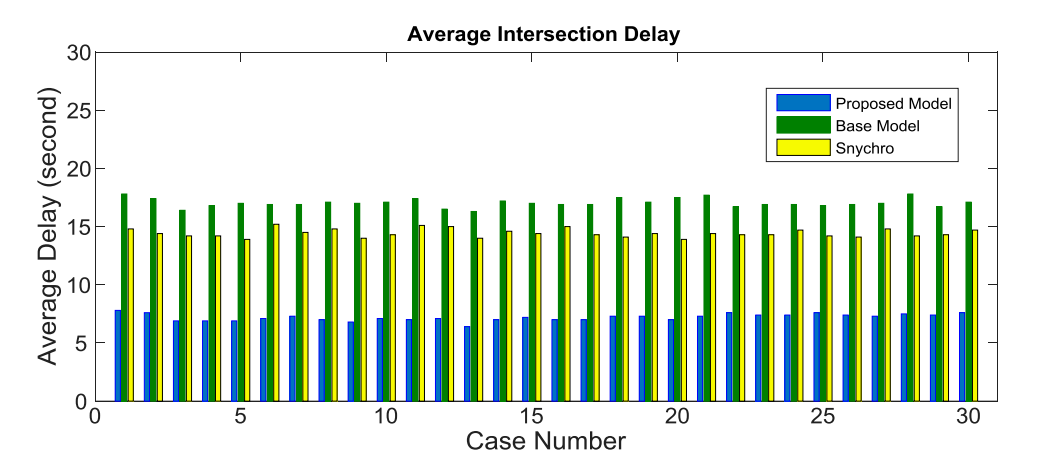


Figure 22. Comparison of superstreet average delay with three different signal designs.

queue constraints. To further evaluate the necessity of specified queue constraints, the maximum queues under different signal plans were collected from VISSIM simulations. The comparison results confirm that the proposed model can consistently outperform the other two models with the shortest queue length.

#### 6. Conclusions

To promote the efficiency of a signalized Superstreet, this study has employed the Mixed-Integer-Linear-Programming (MILP) model to generate the optimal signal plan, and the interactive two-stage solution algorithm. The first stage seeks to find the best cycle length for all sub-intersection, whereas the second stage optimizes the offsets with the objective of concurrently maximizing the bandwidth and minimizing the total delays of minor road drivers. The results of extensive simulation investigations with field data have confirmed that the proposed model clearly outperforms the conventional design methods, such as Synchro, to prevent the queue spillbacks and delay reduction. The comparison results between the proposed model and the base model have further justified the effectiveness of the embedded constraints for the queues and the delays.

Future extension of this research will focus on investigating the signal coordination between a Superstreet and its' neighboring intersections along the same corridor. The purpose is to ensure that the computed offsets and bandwidths can precisely accommodate the need of all heavy flows from different directions. Another direction lies on exploring the impacts of the signal plan from the neighboring intersections on the queue formations within a Superstreet.

#### **Disclosure statement**

No potential conflict of interest was reported by the authors.

#### **Funding**

This study is sponsored by Maryland State Highway Administration to the ATTAP program at the University of Maryland, College Park [grant number SP909B4H].



#### References

- Aboudolas, K., and N. Geroliminis. 2013. "Perimeter and Boundary Flow Control in Multi-Reservoir Heterogeneous Networks." *Transportation Research Part B: Methodological* 55: 265–281.
- Allsop, R. E. 1992. "Evolving Application of Mathematical Optimisation in Design and Operation of Individual Signal-Controlled Road Junctions." In *Mathematics in Transport and Planning and Control*, 1–24. Oxford: Clarendon Press.
- Chang, E. C. P., S. L. Cohen, C. C. Liu, et al. 1988. "MAXBAND-86: Program for Optimizing Left Turn Phase Sequence in Multi-Arterial Closed Networks." *Transportation Research Record* 1181: 61–67.
- Christofa, E., K. Ampountolas, and A. Skabardonis. 2016. "Arterial Traffic Signal Optimization: A Person-Based Approach." *Transportation Research Part C: Emerging Technologies* 66: 27–47.
- Gartner, N. H., S. F. Assmann, F. Lasaga, and D. L. Hou. 1991. "A Multi-Band Approach to Arterial Traffic Signal Optimization." *Transportation Research Part B: Methodological* 25 (1): 55–74.
- Gartner, N. H., and C. Stamatiadis. 2002. "Arterial-based Control of Traffic Flow in Urban Grid Networks." *Mathematical and Computer Modelling* 35 (5-6): 657–671.
- Gartner, N. H., and C. Stamatiadis. 2004. "Progression Optimization Featuring Arterial-and Route-Based Priority Signal Networks." *Journal of Intelligent Transportation Systems* 8 (2): 77–86.
- Hadi, M. A., and C. E. Wallace. 1993. "Hybrid Genetic Algorithm to Optimize Signal Phasing and Timing." *Transportation Research Record* 1421: 104–112.
- Haley, Rebecca, Sarah Ott, Joseph Hummer, Robert Foyle, Christopher Cunningham, and Bastian Schroeder. 2011. "Operational Effects of Signalized Superstreets in North Carolina." *Transportation Research Record: Journal of the Transportation Research Board* 2223: 72–79.
- Heydecker, B. G. 1992. "Sequencing of Traffic Signals." In *Mathematics in Transport and Planning and Control*, edited by J. D. Griffiths, 57–67. Oxford: Clarendon Press.
- Heydecker, B. G., and I. W. Dudgeon. 1987. "Calculation of Signal Settings to Minimise Delay at a Junction." In *Proceedings of the 10th International Symposium on Transportation and Traffic Theory, MIT, July*, 159–178. New York: Elsevier.
- Hughes, W., R. Jagannathan, D. Sengupta, and J. E. Hummer. 2010. Alternative intersections/interchanges: informational report (AlIR) (No. FHWA-HRT-09-060).
- Hummer, J. E. 1998. "Unconventional Left-Turn Alternatives for Urban and Suburban Arterials-Part One." *ITE Journal* 68: 26–29.
- Hummer, J. E., R. L. Haley, S. E. Ott, R. S. Foyle, and C. M. Cunningham. 2010. Superstreet Benefits and Capacities (No. FHWA/NC/2009-06).
- Hummer, J., B. Ray, A. Daleiden, P. Jenior, and J. Knudsen. 2014. Restricted crossing U-turn informational guide (No. FHWA-SA-14-070).
- Improta, G., and G. E. Cantarella. 1984. "Control System Design for an Individual Signalized Junction." Transportation Research Part B: Methodological 18: 147–167.
- Keyvan-Ekbatani, M., A. Kouvelas, I. Papamichail, and M. Papageorgiou. 2012. "Exploiting the Fundamental Diagram of Urban Networks for Feedback-Based Gating." *Transportation Research Part B: Methodological* 46 (10): 1393–1403.
- Keyvan-Ekbatani, M., M. Papageorgiou, and I. Papamichail. 2013. "Urban Congestion Gating Control Based on Reduced Operational Network Fundamental Diagrams." *Transportation Research Part C: Emerging Technologies* 33: 74–87.
- Kim, M., G. L. Chang, and S. Rahwanji. 2007. Unconventional arterial intersection designs initiatives. In IEEE Conference on Intelligent Transportation Systems, Seattle.
- Li, J. Q. 2014. "Bandwidth Synchronization Under Progression Time Uncertainty." *IEEE Transactions on ITS* 15 (2): 1–11.
- Litter, J. D. C., M. D. Kelson, and N. H. Gartner. 1981. "MAXBAND: A Program for Setting Signals on Arteries and Triangular Networks." *Transportation Research Record* 795: 40–46.
- Little, J. D. C., V. Martin B, and T. Morgan J. 1966. "The Synchronization of Traffic Signals by Mixed-Integer Linear Programming." *Operations Research* 14: 568–594.
- Liu, H. 2014. Effects of Crossover Distance on Performance of Super Street (Doctoral dissertation, Texas Southern University).



- Liu, Y., and G. L. Chang. 2011. "An Arterial Signal Optimization Model for Intersections Experiencing Queue Spillback and Lane Blockage." *Transportation Research Part C: Emerging Technologies* 19 (1): 130–144.
- Lo, H. 1999. "A Novel Traffic Signal Control Formulation." *Transportation Research, Part A* 44: 436–448. Lo, H. 2001. "A Cell-Based Traffic Control Formulation: Strategies and Benefits of Dynamic Timing Plan." *Transportation Science* 35: 148–164.
- Moon, J. P., Y. R. Kim, D. G. Kim, and S. K. Lee. 2011. "The Potential to Implement a Superstreet as an Unconventional Arterial Intersection Design in Korea." *KSCE Journal of Civil Engineering* 15 (6): 1109–1114.
- Naghawi, H., A. AlSoud, and T. AlHadidi. 2018. "The Possibility for Implementing the Superstreet Unconventional Intersection Design in Jordan." *Periodica Polytechnica Transportation Engineering* 46 (3): 122–128.
- Naghawi, H. H., and W. I. A. Idewu. 2014. "Analysing Delay and Queue Length Using Microscopic Simulation for the Unconventional Intersection Design Superstreet." *Journal of the South African Institution of Civil Engineering* 56 (1): 100–107.
- Ott, S. E., R. L. Haley, J. E. Hummer, R. S. Foyle, and C. M. Cunningham. 2012. "Safety Effects of Unsignalized Superstreets in North Carolina." *Accident Analysis & Prevention* 45: 572–579.
- Park, B., C. J. Messer, and T. Urbanik. 1999. "Traffic Signal Optimization Program for Oversaturated Conditions: Genetic Algorithm Approach." *Transportation Research Record* 1683: 133–142.
- Reid, J. D., and J. E. Hummer. 1999. "Analyzing System Travel Time in Arterial Corridors with Unconventional Designs Using Microscopic Simulation." *Transportation Research Record* 1678: 208–215.
- Reid, J. D., and J. E. Hummer. 2001. "Travel Time Comparisons Between Seven Unconventional Arterial Intersection Designs." *Transportation Research Record No. 01-2957* 1751: 56–66.
- Robertson, D. I. 1969. TRANSYT: a traffic network study tool. RRL Report LR 253, Road Research Laboratory, England.
- Stamatiadis, C., and N. H. Gartner. 1996. "MULTIBAND-96: A Program for Variable-Bandwidth Progression Optimization of Multiarterial Traffic Networks." *Transportation Research Records*, 1554, 9–17.
- Stevanovic, A., P. T. Martin, and J. Stevanovic. 2007. "VisSim-based Genetic Algorithm Optimization of Signal Timings." *Transportation Research Record: Journal of the Transportation Research Board* 2035: 59–68.
- Sun, C., P. Edara, C. Nemmers, and B. Balakrishnan. 2016. *Driving Simulator Study of J-Turn Acceleration/Deceleration Lane and U-Turn Spacing (No. cmr 16-018)*. Ames, IA: Midwest Transportation Center.
- Thompson, C. D., and J. E. Hummer. 2001. Guidance on the Safe Implementation of Unconventional Arterial Designs (No. Draft Final Report).
- Tian, Z., and T. Urbanik. 2007. "System Partition Technique to Improve Signal Coordination and Traffic Progression." *Journal of Transportation Engineering* 133 (2): 119–128.
- Tully, I. M. 1976. Synthesis of sequences for traffic signal controllers using techniques of the theory of graphs. Ph.D. Thesis, University of Oxford.
- Wallace, C. E., K. G. Courage, D. P. Reaves, G. W. Shoene, G. W. Euler, and A. Wilbur. 1988. *TRANSYT-7F User's Manual: Technical Report*. Gainesville, FL: University of Florida.
- Wong, C. K., and S. C. Wong. 2003. "Lane-based Optimization of Signal Timings for Isolated Junctions." *Transportation Research Part B: Methodological* 37 (1): 63–84.
- Wong, S. C. 1996. "Group-based Optimization of Signal Timings Using the TRANSYT Traffic Model." Transportation Research Part B: Methodological 30: 217–244.
- Xu, L., X. Yang, and G. L. Chang. 2017. "Computing the Minimal U-Turn Offset for an Unsignalized Superstreet." *Transportation Research Record: Journal of the Transportation Research Board* 2618: 48–57.
- Xuan, Y., C. F. Daganzo, and M. J. Cassidy. 2011. "Increasing the Capacity of Signalized Intersections with Separate Left Turn Phases." *Transportation Research Part B: Methodological* 45 (5): 769–781.
- Yagar, S. 1975. "Minimizing Delay at a Signalized Intersection for Time-Invariant Demand Rates." *Transportation Research* 9: 129–141.



- Yang, X., G. L. Chang, and S. Rahwanji. 2014. "Development of a Signal Optimization Model for Diverging Diamond Interchange." Journal of Transportation Engineering 140 (5): 04014010.
- Yang, X., Y. Cheng, and G. L. Chang. 2015. "A Multi-Path Progression Model for Synchronization of Arterial Traffic Signals." Transportation Research Part C: Emerging Technologies 53: 93–111.
- Yun, I., and B. Park. 2006. "Application of Stochastic Optimization Method for an Urban Corridor." In *Proceedings of the Winter Simulation Conference, Monterey, CA, December 3–6,* 1493–1499.
- Zhang, C., Y. Xie, N. H. Gartner, C. Stamatiadis, and T. Arsava. 2015. "AM-band: an Asymmetrical Multi-Band Model for Arterial Traffic Signal Coordination." Transportation Research Part C: Emerging *Technologies* 58: 515–531.
- Zhao, J., W. Ma, K. L. Head, and X. Yang. 2015. "Dynamic Turning Restriction Management for Signalized Road Network." Transportation Research Record: Journal of the Transportation Research Board 2487: 96-111.